The Finite Element Model to Simulate Dynamic Fracture of Initially Intact Media, Dynamic Crack Initiation, Propagation and Arrest

Vladimir Bratov[1a], Yuri Petrov[1b], Alexander Utkin[2c]

[1] Institute of Problems of Mechanical Engineering of the Russian Academy of Sciences, V.O., Bolshoj pr., 61, 199178, St. Petersburg, Russia

[2] St.- Petersburg state University, Universitetsky prospekt, 28, 198504, Peterhof, St. Petersburg, Russia

[a]vladimir@bratov.com, [b]yp@yp1004.spb.edu, [c]a.utkin@udaw.com.ru

Keywords: Dynamic fracture, incubation time approach, SMART1, crack growth, crack arrest

Application of the Incubation Time Approach in Numerical Simulations of Dynamic Fracture

As shown in [1] the incubation time criterion [2], is able to describe crack initiation in dynamic conditions. General form of the criterion for rupture at a point x at time t reads:

$$\frac{1}{\tau}\int_{t-\tau}^{t}\frac{1}{d}\int_{x-d}^{x}\sigma(x^*,t^*)dx^*dt^* \geq \sigma_c , \qquad (1)$$

where τ is the microstructural time of a fracture process (or fracture incubation time) – a parameter characterizing the response of the material on applied dynamical loads (i.e. τ is constant for a given material and does not depend on problem geometry, the way a load is applied, the shape of a load pulse and its amplitude). d is the characteristic size of a fracture process zone and is constant for the given material and chosen scale. σ is stress at a point, changing with time and σ_c is its critical value (ultimate stress or critical tensile stress found in quasistatic conditions). x^* and t^* are local coordinate and time.

Assuming

$$d = \frac{2}{\pi}\frac{K_{IC}^2}{\sigma_c^2} , \qquad (2)$$

where K_{IC} is a critical stress intensity factor for mode I loading (mode I fracture toughness), measured in quasistatic experimental conditions. It can be shown that within the framework of linear fracture mechanics, for case of fracture initiation in th tip of an existing crack, loaded by mode I, (1) is equivalent to:

$$\frac{1}{\tau}\int_{t-\tau}^{t}K_I(t^*)dt^* < K_{IC} . \qquad (3)$$

Condition Eq. 2 arises from the requirement that Eq. 1 is equivalent to Irwin's criterion ($K_I \geq K_{IC}$), in case of $t \to \infty$.

As it was shown in many previous publications, criterion (Eq.3) can be successfully used to predict fracture initiation for brittle solids (ex. [3,4]). Along with prediction of initiation of dynamically loaded cracks incubation time criterion is able to predict dynamic crack propagation, arrest, reinitiation and even fracture of initially intact media. The criterion (Eq.3), while able to predict dynamic crack initiation, cannot be used to predict crack or fracture development in

dynamic conditions. The main reason for this is that time dependency of a stress intensity factor in the tip of a crack moving at high speeds does not directly reflect the history of stress-strain fields in the vicinity of a current crack tip location as, at preceding times, crack tip was located at distant (and usually very distant) points of a body. This was also discussed by Ma and Freund [5] and Ravi-Chandar and Knauss [6].

Though criterion using stress intensity factor (Eq.3) is easier to use when simply describing crack initiation, general form of the incubation time criterion (Eq.1) was used even to assess early stages of fracture development. In this work examples on how the incubation time approach, being incorporated into finite element computational codes, can be used to predict fracture initiation, propagation and arrest in real experimental conditions are given.

Classical experiments of Ravi-Chandar and Knauss

Incubation time criterion was used to predict dynamic crack development in the classical fracture dynamics experiments reported by Ravi-Chandar and Knauss in 1984 [7]. In these experiments a rectangular sample with a cut simulating a crack is loaded by applying an intense load pulse to the crack faces. Fig. 1 gives an approximation of the load applied to the crack faces.
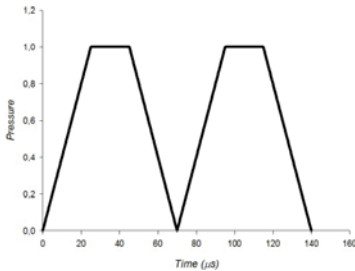

Figure 1

Temporal shape of pressure pulse released at experiments by Ravi-Chandar and Knauss (1984a)

Behavior of the loaded sample is described by the Lame equations:

$$\rho u_{i,tt} = (\lambda + \mu) u_{j,ji} + \mu u_{i,jj} \ ,$$

where "," refers to the partial derivative with respect to time and spatial coordinates. ρ is the mass density, and the indices i and j assume the values 1 and 2. Displacements are given by u_i in the directions x_i respectively. t stands for time, λ and μ are Lame constants. Stresses are coupled with strains by Hooke's law:

$$\sigma_{ij} = \lambda \delta_{ij} u_{k,k} + \mu(u_{i,j} + u_{j,i}) \ .$$

where σ_{ij} represents components of the stress tensor, δ_{ij} is the Kronecker delta assuming value of 1 for $i=j$ and 0 otherwise. At $t=0$ the sample is stress free and velocity field is zero everywhere in the body:

$$\sigma_{ij}\big|_{t=0} = u_{,t}\big|_{t=0} = 0 \ . \tag{6}$$

Crack faces are free from tractions:

$$\sigma_{21}\big|_{x_1<0,x_2=0} = 0 \ . \tag{7}$$

The load applied to the crack faces is given by:

$$\sigma_{22}\big|_{x_1<0,x_2=0} = Af(t) \ . \tag{8}$$

Where $f(t)$ is given graphically in Fig. 1 and A is the amplitude of the load. The authors create a pressure pulse, constant over the cut.

Unfortunately, in the article by Ravi-Chandar and Knauss there is no information about the amplitude of pressure created in the presented experiments [7].

To check applicability of Eq.1 to describe dynamic crack propagation experimental conditions of [7] were modeled utilizing the finite element method.

Finite element formulation

In order to obtain a closed mathematical description of the dynamic fracture problem Eqs.4-8 is supplemented with fracture criterion Eq.1. Due to symmetry, we suppose that the crack can propagate only along the x_1 axis. When condition (Eq. 1) is fulfilled somewhere along a crack path, we suppose creation of a new surface in that point.

The problem defined by Eqs.1,4-8 is solved numerically utilizing the finite element method. ANSYS finite element package was used to implement (4)-(8), and the fulfillment of condition (1) was checked by an external program after each time step [8].

Rectangular 4-node elements were used to mesh a body. The size of elements along the crack path was taken to be exactly $d = \dfrac{2}{\pi} \dfrac{K_{IC}^2}{\sigma_c^2}$. Using the symmetry of the problem across the x_1 axis the problem was solved only for the upper half of the sample. Dimensions of the modeled sample were the same as in the experiments of Ravi-Chandar and Knauss [7].

Density, $\rho, \dfrac{kg}{m^3}$	1230
Young's modulus, E, MPa	3900
Poisson's ratio, ν	0.35
Critical stress intensity factor, $K_{IC}, Mpa\sqrt{m}$	0.48
Ultimate tensile stress, σ_c, MPa	48
Incubation time of fracture, τ, μs	9

Table 1
Properties of Homalite-100 used in numerical simulations

Due to the symmetry of the problem the crack path should follow the x_1-axis. Nodes along the path are subjected to symmetrical boundary conditions up to the moment when the condition (Eq.1) is satisfied at a particular node (node movements in the vertical direction are restricted). At this moment the restriction on movement of the particular node is removed and a new surface is created. The technique used is similar to the node release technique.

The shape of the pressure pulse applied to the crack faces is given by Fig. 1, and its amplitude A is alternated in simulations. Material parameters typical for Homalite-100, used in the experiments of Ravi-Chandar and Knauss, were used in the calculations.

These parameters are presented in Table 1.

Solution Results

After the stated problem is solved by the FEM package, together with an external program controlling crack propagation, information about K_I time dependency and the crack extension history is provided for further analysis. $K_I(t)$ is computed using the asymptotic behavior of the stress field surrounding the crack tip.

It was observed that, depending on the amplitude of the applied pressure pulse A, three different modes of crack propagation are possible. The first one is trivial – amplitude that is too low results in no crack extension. The second one is the mode observed by Ravi-Chandar and Knauss [7]. The crack starts propagating at a constant speed. Then it arrests, due to the energy flow into the crack tip which is no longer sufficient for its propagation. When the energy from the second trapezoid of the loading pulse approaches the crack tip region, the crack reinitiates and starts propagating at approximately the same speed as in the first stage of its extension.

Further increase of load amplitude *A* results in a propagation mode change. Now the crack is initiated, propagates at some constant speed, and when the energy from the second part of the

loading pulse is delivered to the crack tip region the crack is accelerated and continues propagation at a higher speed.

By adjusting the pressure amplitude *A*, it was found that amplitudes around 5 *MPa* result in crack extension histories very close to those observed by Ravi-Chandar and Knauss [7]. In Fig. 2, the computational result for *A*=5.1 *MPa* is compared to one of the experiments [7].
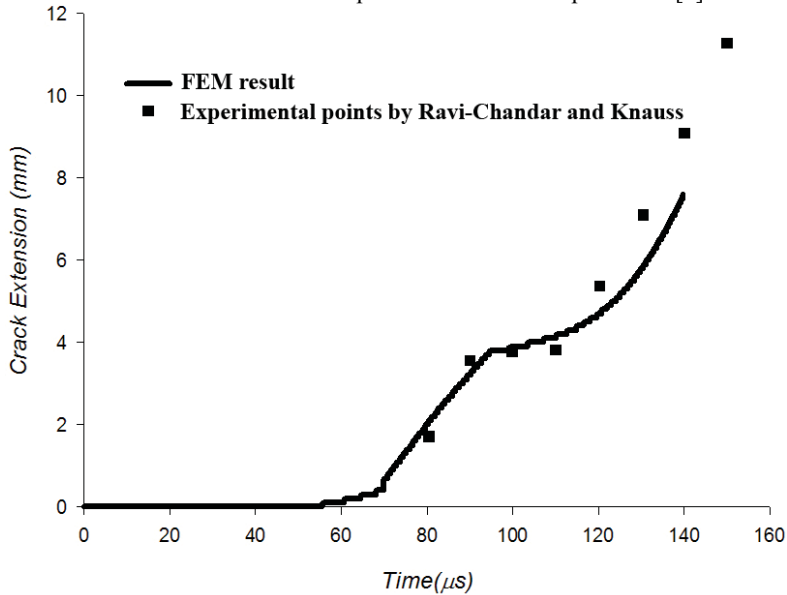

Figure 2

Crack extension history. Comparison of FEM calculation with experimental data points of Ravi-Chandar and Knauss [7]

Conclusions on dynamic crack simulations

It has been shown that, solving the dynamic problem of linear elasticity by FEM and criterion Eq.1 being used to assess critical conditions for crack advancement, the propagation of dynamically loaded cracks can be predicted. It has also been shown that criterion (Eq.1) with *d*, chosen from the condition of coincidence of Eq.1 with Irwin's criterion in static conditions can be used to describe dynamic crack initiation, propagation and arrest.

Criterion Eq.1, unlike Eq.3, which is applicable only to crack initiation, can also be used as the condition for crack propagation and arrest. In the presented model Eq.1 is used as a condition for node release. This criterion does not even require the presence of a crack. Thus, the condition for crack propagation and arrest appears automatically. The crack propagates whilst Eq.1 is fulfilled for nodes ahead of the moving crack tip; otherwise the crack arrests.

Using a similar method one can model cracks that change their direction of propagation and even branch. In this case Eq.1 should be applied not only to stresses acting perpendicular to the x_1 direction, as is done in the presented research, but in all the possible directions surrounding the x^* point.

According to the incubation-time based approach (see [9 or [2]), in combination with a variety of widely known experimental observations, the critical stress intensity factor at the crack initiation moment under high rate loads may, depending on the experimental geometry, loading conditions and history, either be noticeably smaller or greater than K_{IC} .

Application of the incubation-time based approach allows one to describe all variety of experimentally observed effects in fracture dynamics. An important consequence of this approach is that it provides an effective way of testing dynamic strength by direct measurement of τ, a parameter intrinsic to the material and not dependent on experimental geometry or the way the load is applied [10]. This provides a tool that can be directly incorporated into practical engineering.

Simulation of SMART1 satellite impacting the moon surface

As shown above, incubation time fracture criterion Eq.1 can be applied to study the evolution of the fracture process. This includes not only a simulation of crack propagation in bodies with initial cracks but also fracture of initially intact media. In this section an example of how the incubation time approach can be incorporated into the finite element code in order to simulate fracture of initially intact media is presented. The example is the simulation of conditions of satellite SMART1 lunar impact conducted by European Space Agency year 2006 [11,12] is presented. Aim of the simulation is to compare dimensions of crater created due to SMART1 contact to the moon surface to results received using finite element method utilizing incubation time criterion as the critical rupture condition.

An approach similar to one used to predict crack propagation in experiments of Ravi-Chandar and Knauss[7], can be used to simulate fracture of initially intact media. The difference is, that in this case finite element code should trace fracture condition fulfillment in all the nodes of the modeled sample and be able of creating a new surface in respective points once rupture criterion is implemented somewhere in the body. 2-D problem with rotational symmetry is solved. Quadratic 4-node elements are used. Dimensions of every element is exactly d times d (where d is given by Eq.2).

For internal points of the fractured sample condition Eq.1 can be written:

$$\frac{1}{\tau}\int_{t-\tau}^{t}\sigma_{ii}(t^*)dt^* \geq \sigma_c ,$$ (9)

where i assumes values 1 and 2. Repeating indices does not dictate summation in this case. Spatial integration is removed, because the stress in the respective direction calculated by finite element program is already a mean value over size d (as d is the element size being used).

The problem is solved for a half-space $x_2<0$. Eqs.4-6 give state equations and initial conditions for the half-space. Half-space representing the moon had following material properties: σ_c=10.5 MPa, $K_{IC} = 2.94 MPa\sqrt{m}$, $\tau = 80\mu s$, E =60 GPa, ρ=2850 kg/m^3, ν=0.25 typical for earth basalt. This results in d=5 cm. Half-space is impacted by a cylinder with diameter of 1 meter and height of 1 meter. Density for the cylinder is chosen so that its mass is the same as the one of SMART1 satellite. We suppose material of cylinder is linear elastic and has no possibility to fracture. SMART1 satellite had a form close to cubic with side of 1meter and had a mass of 366 kg. SMART1 impacted the moon surface at a speed of approximately 2000 m/s. In finite element formulation the cylinder was given an initial speed of 2000 m/s prior its contact to the half-space boundary. Figure 9 gives an overview of the finite element model. Size of the sample, representing the half-space is chosen from a condition that the waves reflected from the sample boundaries are not returning to the region where the crater is formed in the process of the simulation.

ANSYS finite element package [8] was used to solve the stated problem. Control of the fracture condition (Eq. 9) fulfillment in all of the sample points and new surface creation when rupture criterion is implemented was carried out by a separate ANSYS ADPL subroutine.

Figure 3 shows the sample state after the simulation is finished. Damage localized at down part of the sample is due to finite dimensions of a sample and represent cleavage fracture that occurred after compressive waves are reflected from lower boundary. In figure 4 locations of nodes where the fracture occurred are marked. This gives a possibility to assess dimensions of crater that is formed after the SMART1 impact. Damaged zone is found to be about 10 meters in diameter and about 3 meters deep. Zone where the material is fully fragmented (crater formed) can be assessed having 7-10 meters in diameter and 3 meters deep. This result is coinciding with ESA estimations of dimensions of crater formed due to SMART1 impact [11,12].
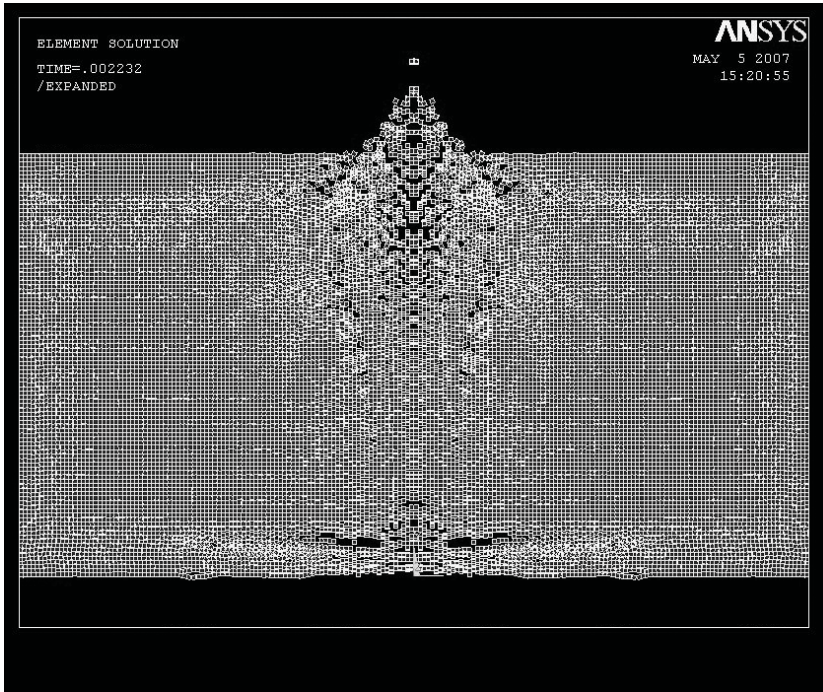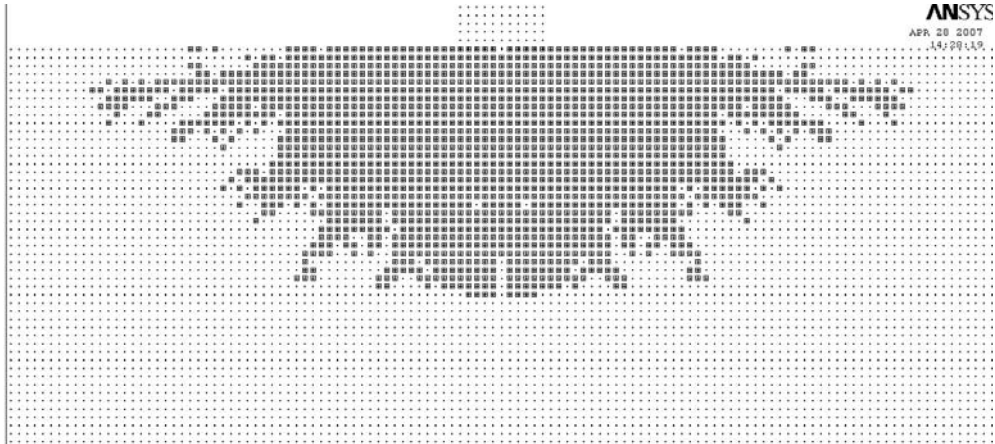

Figure 3
Sample after impact

Figure 4
Locations of ruptured nodes

Conclusions

Incubation time fracture criterion has a wide area of applicability. As real dynamic fracture problems rarely can be solved analytically, the majority of applications require numerical simulations. In this connection incubation time approach has a significant advantage – it can be applied for correct description of both quasistatic and dynamic fracture, so one does not have to use separate criteria for different load rates. It is shown that using incubation time criterion incorporated into finite element code a correct description of dynamic fracture initiation, dynamic crack propagation and fracture of initially fractured media is possible. It is remarkable that staying within the framework of linear elastic fracture mechanics, it is possible to predict all the variety of effects inherent in dynamic fracture. And all this is possible while utilizing a rather simple fracture model, not incorporating complicated cohesive laws. The same approach can be used to model dynamic crack arrest, dynamic cleavage, etc.

References

[1]   Morozov, N., Petrov, Y. (2000) Dynamics of Fracture. Springer-Verlag, Berlin-Hidelberg-New York

[2]   Petrov, Y.V., Morozov, N.F. (1994) On the modeling of fracture of brittle solids. Journal of Applied Mechanics 61:710-712

[3]   Petrov, Y.V., Morozov, N.F., Smirnov, V.I. (2003) Structural micromechanics approach in dynamics of fracture. Fatigue and fracture of Engineering Materials and Structures 26:363-372

[4]   Petrov, Y., Sitnikova, E. (2005) Temperature dependence of spall strength and the effect of anomalous melting temperatures in shock-wave loading. Technical Physics 50:1034-1037

[5]   Ma, C.C., Freund, L.B. (1986) The Extent Of The Stress Intensity Factor Field During Crack Growth Under Dynamic Loading Conditions. ASME Journal of Applied Mechanics 53:303-310

[6]   Ravi-Chandar, K., Knauss, W.G. (1987) On the characterization of the transient stress field near the tip of a crack. Journal of Applied Mechanics 54:72:78

[7]   Ravi-Chandar, K., Knauss, W.G. (1984) An experimental investigation into dynamic fracture: I. Crack initiation and arrest. International Journal of Fracture 25:247-262

[8]   ANSYS (2006) User's Guide, Release 11.0. ANSYS Inc., Pennsylvania, USA

[9]   Petrov, Y.V. (1991) On "Quantum" Nature of Dynamic Fracture of Brittle Solids. Doklady Akademii Nauk USSR 321:66-68

[10]   Petrov, Y.V. (2004) Incubation time criterion and the pulsed strength of continua: fracture, cavitation, and electrical breakdown. Doklady Physics 49:246-249

[11]   ESA (2006a) ESA Press Release 31-2006. Impact landing ends SMART-1 mission to the Moon. http://www.esa.int/esaCP/SEM7A76LARE_index_0.html.

[12]   ESA (2006b) Intense final hours for SMART-1, http://www.esa.int/esaCP/SEMV386LARE_index_0.html

[13]   Hopkinson, J. (1901) Original Papers, Cambridge University Press.